Effects of Bending on Asymmetric and Curved Beams

Course: Structural Mechanics and Dynamics 3

Semester: Autumn 2025

Exam No. B251192

Experiments conducted in **Group 03** on **Tuesday, 21st October 2025**.

Report Submitted on **23/11/2025**

CONTENTS

SECTION 1 – BENDING OF AN ASYMMETRIC BEAM

SECTION 2 – BENDING OF A CURVED BEAM

SECTION 3 - APPENDICES

SECTION 1 – BENDING OF AN ASYMMETRIC BEAM

This section of the laboratory report discusses the experimental findings when an asymmetric L-shaped beam is rotated about an axis and subjected to a bending moment exerted by a load at the tip of the beam.

1.1 – CONTEXTUAL DESCRIPTION AND SETUP

Figure 1.1.1 (right) is a simplified hand-drawn diagram of the experimental setup.

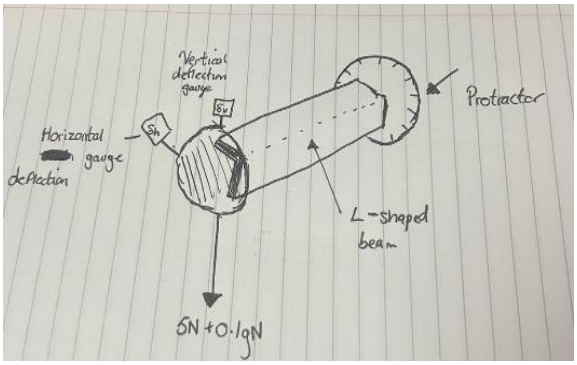

Figure 1.1.1 – Simplified diagram of L-beam

Any uniform beam with an arbitrary cross-section will have principal axes that intersect at the centroid when subjected to a bending moment exerted by a load (Ma, 2024, p.168-170). In the case of the L shaped beam, the centroid of the cross-section can be found by calculating the weighted average of cross-sections for the individual rectangles in the compound shape (Ma, 2024, p. 433). Awareness of the locations of the principal axes is a critical factor in structural design, as these permit the calculations of maximum and minimum bending stresses in a section.

A uniform L-shaped beam of length 500mm was fixed at one end in a cantilever configuration, with a protractor to determine the beam's angle to the vertical. A vertical load (attached at a length of 540mm) of 5N was applied via a hook - itself applying a downward force of 0.981N – at the tip of the beam. Deflection gauges were placed to measure the horizontal and vertical deflection of the beam upon application of the load. Loading occurred through the centroid to prevent additional torsional stresses that influence the stress distribution in the beam. Measurements of the cross-section's dimensions were taken using a digital micrometer with a resolution of 0.01mm. The angle of rotation was manually read once with a protractor, with an estimated error per reading of 1º.

1.2 – DESCRIPTION OF ANALYTICAL PROCESS

Measurements were taken of the height h = 27.01 ± 0.01 mm of one of the vertical legs, the length l = 24.97 ±0.01mm of the perpendicular leg and the thickness t = 3.51 ± 0.11mm of the beam (measured on both legs). For each reading of horizontal and vertical deflection, the beam was to be rotated by 10º with both gauges tared before the load was applied. The horizontal and vertical deflections were then read once per angle, to be plotted against the loading angle to determine the position of the principal axes. The beam in pure plane bending (i.e. aligned with the principal axis) will experience *no* horizontal deflection, and a *maximum/minimum* vertical deflection at the angles where the *area cross-moment of inertia is zero*. Equations {B.1.1} through {B.1.6} (available in Appendix B) were used to calculate these values.

All plots in the report were obtained by writing Python scripts that are available in the linked GitHub repository in Appendix C. Error in the empirical readings is difficult to determine as the deflection for each angle was only measured once; instrumental resolution uncertainty is minimal for the sake of the plots and is not included.

1.3 – RESULTS

The calculated angle between the geometric axes of the beam and its principal axes is **42.429⁰** *anticlockwise from the horizontal axis*. Figure 1.3.1 consists of two plots side by side which display points for the empirical data values for both horizontal and vertical deflections, alongside 4th order polynomial least squares regressions (a sufficient Taylor Series approximation for one period). Figure 1.3.2 tabulates the values indicated in red on the plot with theoretical discrepancies.

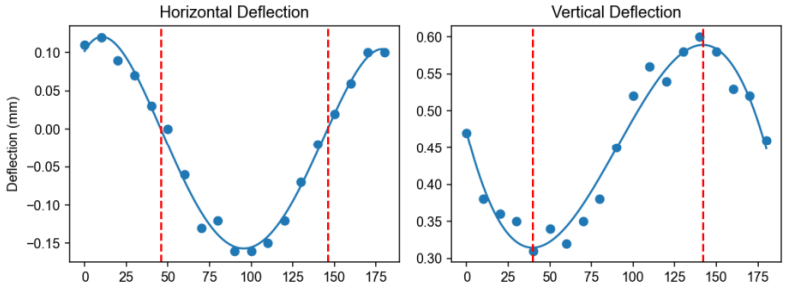

Figure 1.3.1 – Plots for horizontal and vertical deflections with polynomial regressions and principal axes values (in red)

THEORETICAL = 42.429⁰, 132.429⁰	Angle 1	Angle 2
Horizontal Deflection	***45.796⁰***	***145.928⁰***
Error to Theoretical	***7.9%***	***10.2%***
Vertical Deflection	***39.570⁰***	***141.942⁰***
Error to Theoretical	***-6.7%***	***7.2%***

Figure 1.3.2 – Table of results for principal axes

1.4 – CONCLUSIONS AND DISCUSSIONS

Analysis of results as discussed above yielded the following conclusions:

- Horizontal deflection varied sinusoidally, and the theoretical angle of the principal axis (where equal to 0) to the horizontal exhibited discrepancies of 7.9% and 10.2% respectively
- Vertical deflection varied sinusoidally, where the angles of minimum and maximum deflection disagreed with the location of the theoretical principal axes by -6.7% and 7.2% respectively
- Discrepancies between theoretical and empirical values are likely caused by the uncertainty of having not taken multiple readings
- The difference between the two angles for both deflections is greater than expected – use of a manual protractor to read angle may have compounded additional error in the regression

The coupling between horizontal and vertical deflections is supported by the theory as cited above, due to its asymmetry. This is a necessary consideration for industrial requirements in computing maximum bending stresses. A flaw in the methodology of the experiment was the single readings of the beam's geometry – average values taken by multiple readings along different points is a more accurate method that went unutilised (except the average thickness). Consequently, calculations may have been unduly influenced by incorrect values, with uncertainties much larger than the resolution. An alternative source of error is a centroidal loading misalignment – which would introduce unaccounted torsion and bending.

SECTION 2 – BENDING OF A CURVED BEAM

This section of the laboratory report discusses the experimental findings when a curved beam is subjected to a bending moment exerted by a load at the tip of the beam.

2.1 – CONTEXTUAL DESCRIPTION AND SETUP

Utilisation of Castigliano's Theorem permits the analysis of the horizontal and vertical deflections at the tip of a semi-circular proving ring when a load is applied vertically from the top, according to the following schematic:
A semi-circular proving ring was fixed in a cantilever configuration at the bottom, and a varying gravitational load (attached to a hook with weight 0.981N) in increments of 2N was applied from the free end of the beam. Digital gauges were attached to the beam to measure the deflections in both horizontal and vertical axes. The weights were attached to the hook, corresponding to a load up to ~10N in increments of 2N where possible, with each weight gradually removed so that multiple readings of deflection in both axes were taken for the same load. The mean of the two readings was then plotted against the load, with error bars plotted for data with heights equal to half the difference between the points.

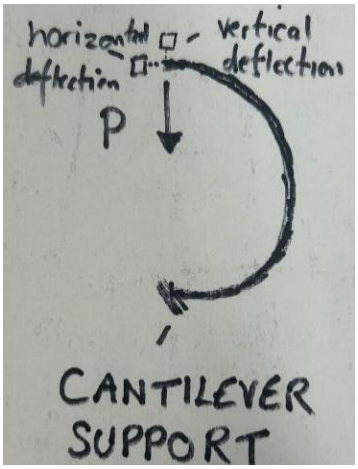

Figure 2.1.1 – Curved Beam Schematic

2.2 – DESCRIPTION OF ANALYTICAL PROCESS

Figure 2.2.1 contains information concerning the dimensions of the semi-circular proving ring alongside their uncertainties due to the instrumental resolution of the micrometer and metre rule:

Width	Thickness	Inner Diameter
25.10 ± 0.01mm	3.40 ± 0.01mm	290.5 ± 0.5mm

Figure 2.2.1 – Tabulated data for beam dimensions

This datasheet was imported into a Python file, where the theoretical deflections were calculated using equations {B.2.1} and {B.2.2} for a linear space of loads ranging from 0N to 12N, which are available in Appendix B. Instrument resolution values were then used to calculate the uncertainty of the deflection as a function of the theoretical deflection itself. Relative uncertainties for both deflections were approximated by multiplying the relative uncertainties by the variable's exponent. The overall relative uncertainty for deflection was calculated by summing these values and multiplying by each theoretical deflection datum.

A linear model for least-squares regression was developed for two purposes:

- Find a coefficient of determination indicating the goodness of fit (to support the hypothesis of linearity)
- Experimental value of the slope which provided a measure of the relative percentage error.

A plot each for theoretical horizontal and vertical deflections (alongside lines for their maximum uncertainties) were plotted on the same axes (deflection against load) as the experimental data and their respective linear regression models. Numerical values for each parameter are available in tabulated form in Figure 2.2.1 (above), or in the link to the public GitHub repository for this project – both in Appendix C. The moment of inertia used for the results is calculated in Appendix B.

2.3 – RESULTS

Figures 2.3.1 and 2.3.2 demonstrate the theoretical horizontal and vertical deflections of the setup plotted on the same axes as the obtained experimental data. The plots include the theoretical deflections using the measured parameters in the experiment, with additional plots above and below which add and subtract the deflection error based on the relative error of the measured parameters due to instrument resolution. Details of these calculations are available in Appendix B.

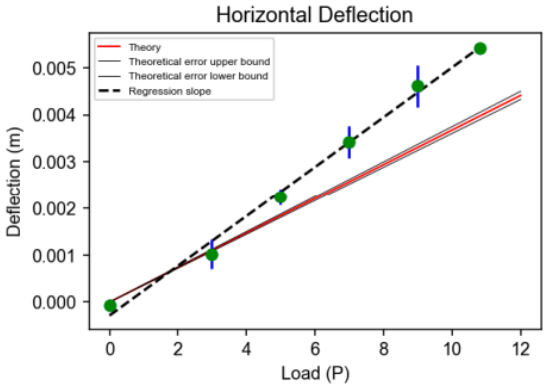

Figure 2.3.1 – Horizontal deflection against load

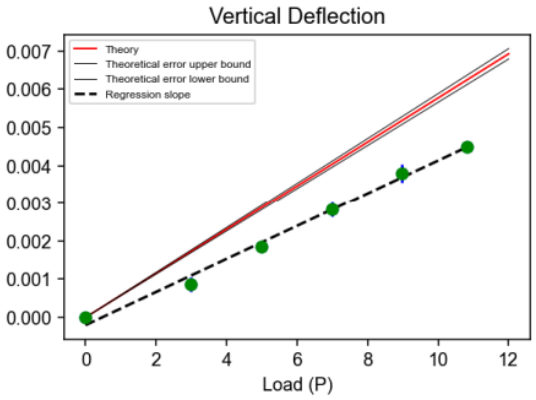

Figure 2.3.2 – Vertical deflection against load

2.4 – CONCLUSIONS AND DISCUSSIONS

Analysis of the experimental results yielded the following conclusions:

- Both horizontal and vertical deflections exhibited proportional relationships to the load applied at the tip: least squares linear regression of the plots yielded R^2 values of greater than 0.99, indicating that a linear model is an excellent predictor for deflection against load.
- There are significant discrepancies in the slopes of the theoretical and experimental data for both deflection plots – comparison of the horizontal and vertical percentage errors in slope found a +43.9% error and a -24.9% error respectively
- Experimental analysis of the relationship demonstrates that the posed hypothesis is supported, in agreement with textbook theory, yet indicates a systematic error either in the experimental process or in the theoretical calculations.
- Unequal unloaded deflections may indicate yielding and an open hysteresis loop

Potential sources of unaccounted error beyond resolution uncertainty include:

- Improperly fixed cantilever support – the equation only holds if there is no rotation nor torsion at the cantilever end – support was assumed to be fixed correctly but was never checked before the experiment began – deflections may
- Loading geometry – the geometric centre of mass may not have aligned with the axis of loading due to all weights not being in direct alignment – this would induce a greater horizontal bending effect than expected due to an induced bending moment through the centroid of the section, causing additional deflection

The results also demonstrate the importance of real-world testing of theoretical systems – a refined experimental process more methodologically focused on reducing errors may validate or undermine the theoretical simulations, a check that could prevent failures of beams in real-world contexts.

APPENDICES

APPENDIX A – RAW DATA SHEETS

Images of the raw datasheets and data frames inputted to the Python program are available below (as *Figures A.1.1* and *A.1.2*). These files are also available in the GitHub repository associated with this report (cited in Appendix C):

Parameters	Value	Error
Height	27.01	0.01
Length	24.97	0.01
Thickness	3.51	0.11
Beam Length	500	0
Load	5.981	0

Angle	Error	Horizontal Deflection	Horz Error	Vertical Deflection	Vert Error
0	1	0.11		0.47	
10	1	0.12	0.012	0.38	0.038
20	1	0.09	0.005	0.36	0.018
30	1	0.07	0.002	0.35	0.012
40	1	0.03	0.001	0.31	0.008
50	1	0	0.000	0.34	0.007
60	1	-0.06	-0.001	0.32	0.005
70	1	-0.13	-0.002	0.35	0.005
80	1	-0.12	-0.002	0.38	0.005
90	1	-0.16	-0.002	0.45	0.005
100	1	-0.16	-0.002	0.52	0.005
110	1	-0.15	-0.001	0.56	0.005
120	1	-0.12	-0.001	0.54	0.005
130	1	-0.07	-0.001	0.58	0.004
140	1	-0.02	0.000	0.6	0.004
150	1	0.02	0.000	0.58	0.004
160	1	0.06	0.000	0.53	0.003
170	1	0.1	0.001	0.52	0.003
180	1	0.1	0.001	0.46	0.003

Figure A.1 – Raw data for Section 1

Offset Weight (N)	Weight	H_D 1 (m)	H_D 2 (m)	Mean H_D (m)	V_D 1 (m)	V_D 2 (m)	Mean V_D (m)	Error in Weight (m	Error in H_D (m	Error in V_D (m
0.000	0.000	-1.50E-04	2.00E-05	-6.50E-05	-5.00E-05	5.00E-05	0.00E+00	0.00E+00	0.00E+00	0.00E+00
2.000	2.981	7.10E-04	1.33E-03	1.02E-03	6.70E-04	1.05E-03	8.60E-04	3.29E-03	3.10E-04	1.90E-04
4.000	4.981	2.08E-03	2.42E-03	2.25E-03	1.77E-03	1.95E-03	1.86E-03	1.97E-03	1.70E-04	9.00E-05
6.000	6.981	3.08E-03	3.77E-03	3.43E-03	2.64E-03	3.02E-03	2.83E-03	1.41E-03	3.45E-04	1.90E-04
8.000	8.981	4.17E-03	5.06E-03	4.62E-03	3.55E-03	4.04E-03	3.80E-03	1.09E-03	4.45E-04	2.45E-04
9.824	10.805	5.45E-03	5.38E-03	5.42E-03	4.50E-03	4.51E-03	4.51E-03	9.08E-04	3.50E-05	5.00E-06

Figure A.2 – Raw data for Section 2

APPENDIX B – CALCULATIONS

SECTION B.1 – CALCULATIONS FOR ASYMMETRIC BEAM

Explicit calculations were performed in both Appendix B and the Python script "experiment 1 - parameters.py", available in the GitHub repository in Appendix C (to ensure accuracy). The parameters used were given in Section 1.2, but are given here for clarity:

Height of Horizontal Leg h_h	Height of Vertical Leg h_v	Thickness t
24.97mm	27.01mm	3.51mm

The centroid in the z and y directions was found by treating the L beam as a composite shape and calculating the weighted average of the centroids. The area and centroid position of the vertical leg were treated to remove the 3.51 x 3.51 overlap at the legs' intersection:

$$\bar{z} = \frac{A_h\overline{z_h} + A_v\bar{z}_v}{A_h + A_v} = \frac{(h_h t)\left(\frac{h_h}{2}\right) + \left((h_v - t)(t)\right)\left(\frac{t}{2}\right)}{t(h_h + h_v - t)} \{\boldsymbol{B.1.1}\}$$

$$\bar{y} = \frac{A_h\overline{y_h} + A_v\overline{y_v}}{A_h + A_v} = \frac{(h_h t)\left(\frac{t}{2}\right) + \left((h_v - t)(t)\right)\left(t + \frac{h_v - t}{2}\right)}{t(h_h + h_v - t)} \{\boldsymbol{B.1.2}\}$$

The area moments of inertia about the z axis and the y axis passing through the centroid were found in a similar method, summing the area moments of inertia of the legs and accounting for their Parallel Axis Theorem offsets:

$$I_Z = \frac{h_h t^3}{12} + (h_h t)(\overline{y_h} - \bar{y})^2 + \frac{t(h_v - t)^3}{12} + \left((t)(h_v - t)\right)(\overline{y_v} - \bar{y})^2 \{\boldsymbol{B.1.3}\}$$

$$I_y = \frac{t h_h^3}{12} + (h_h t)(\overline{z_h} - \bar{z})^2 + \frac{(h_v - t)t^3}{12} + \left((t)(h_v - t)\right)(\overline{z_v} - \bar{z})^2 \{\boldsymbol{B.1.4}\}$$

The value for the cross-section area moment of inertia I_{yz} was calculated using:

$$I_{yz} = \Sigma(A_h(\overline{y_h} - \bar{y})(\overline{z_h} - \bar{z}))\ \{\boldsymbol{B.1.5}\}$$

The position of the principal axes is related to these three values by the equation:

$$\alpha = \frac{-\arctan\left(\frac{2I_{yz}}{I_z - I_y}\right)}{2}\ \{\boldsymbol{B.1.6}\}$$

Treatment of experimental data was conducted in the Python file “experiment 1.py”.

A polynomial regression of the data for both horizontal and vertical deflection used the standard method of least squares regression with 5 calculated parameters. These were converted into SymPy expressions which were then differentiated.

- The roots of the deflection function in the horizontal direction indicated a coincidence with a principal axis
- The roots of the deflection derivative function in the vertical direction indicated a coincidence with a principal axis.

The numerical calculations are as follows (coordinate origin at the bottom left corner of the beam):

CENTROIDS

$$\bar{z} = \frac{A_h\overline{z_h} + A_v\bar{z_v}}{A_h + A_v} = \frac{(24.97 * 3.51)\left(\frac{24.97}{2}\right) + \left((27.01 - 3.51)(3.51)\right)\left(\frac{3.51}{2}\right)}{3.51(24.97 + 27.01 - 3.51)} = 7.28mm$$

$$\bar{y} = \frac{(24.97 * 3.51)\left(\frac{3.51}{2}\right) + \left((27.01 - 3.51)(3.51)\right)\left(3.51 + \frac{27.01 - 3.51}{2}\right)}{3.51(24.97 + 27.01 - 3.51)} = 8.30mm$$

AREA MOMENTS OF INERTIA

$$I_Z = \frac{24.97 * 3.51^3}{12} + (24.97 * 3.51)\left(\frac{3.51}{2} - 8.30\right)^2 + \frac{3.51(27.01 - 3.51)^3}{12}$$
$$+ \left((3.51)(27.01 - 3.51)\right)\left(\left(3.51 + \frac{27.01 - 3.51}{2}\right) - 8.30\right)^2 = 11636mm^4$$

$$I_y = \frac{3.51 * 24.97^3}{12} + (24.97 * 3.51)\left(\frac{24.97}{2} - 7.28\right)^2 + \frac{(27.01 - 3.51)3.51^3}{12}$$
$$+ \left((3.51)(27.01 - 3.51)\right)\left(\frac{3.51}{2} - 7.28\right)^2 = 10527mm^4$$

$$I_{yz} = (24.97 * 3.51)\left(\frac{24.97}{2} - 7.28\right)\left(\frac{3.51}{2} - 8.30\right) + ((27.01 - 3.51) * 3.51)(\frac{3.51}{2}$$
$$- 7.28)(\left(3.51 + \frac{27.01 - 3.51}{2}\right) - 8.30) = -6158mm^4$$

ANGLE OF PRINCIPAL AXES:

$$\alpha = \frac{-\arctan\left(\frac{2(-6158)}{11636 - 10527}\right)}{2} = \boldsymbol{42.429}°$$

SECTION B.2 – CALCULATIONS FOR CURVED BEAM

All reading and manipulation of data was handled in the Python file “experiment 2.py”.

The horizontal and vertical deflections were calculated using the equations obtained from analysis of a semi-circular proving ring using Castigliano’s Theorem of strain energy, obtained from the handbook:

$$\delta_h = \frac{2PR^3}{EI} \{\boldsymbol{B.2.1}\}$$

$$\delta_v = \frac{\pi PR^3}{EI} \{\boldsymbol{B.2.2}\}$$

The moment of inertia of the rectangle used was:

$$I = \frac{bh^3}{12} = 25.1 * \frac{3.40^3}{12} = 82.2mm^4$$

Error was incorporated into the treatment of both theoretical and experimental data using the parameter resolution. A maximum error and minimum error line proportional to the slope itself were added to the plot, alongside error bars for the individual data points based on the uncertainty because of multiple measurements.

Linear regression was also performed on both datasets using the least squares regression technique, and these were added to the plot. This was done so that a discrepancy in slope could be calculated and presented in the conclusions.

APPENDIX C – REASONS AND ASSUMPTIONS

C.1 – REASONS AND ASSUMPTIONS FOR SECTION 1

- The weight of the beam and the induced bending moment due to its own weight will have influenced the deflection values to a certain extent but relative to other sources of error, this influence was negligible and therefore neglected in theoretical considerations – the beam itself was assumed to be massless
- The structure itself was modelled as a lumped section with one degree of freedom, but not as a rigid body as its deformation was the variable being measured
- The modelled system was treated as isolated with no consideration for thermal effects on the structure.

C.2 – REASONS AND ASSUMPTIONS FOR SECTION 2

- The deflection is experienced by section modelled as a thin rectangle at the top of the proving ring with negligible width – this would provide the standard moment of inertia $I = \frac{bh^3}{12}$ with no offset due to the Parallel Axis Theorem as the centroid of the deflected section is coincident with the axis of bending.
- The equation holds for deflection in both directions, as the axis of loading remains constant and perpendicular to the axis of bending.
- Much like the first experiment, the weight of the beam and induced bending moment where the beam would deflect under its own weight was neglected from the calculations
- The section was also modelled to be lumped with one degree of freedom but not as a rigid body, with no consideration for thermal effects which would have been negligible.

APPENDIX D – REFERENCES

Ma, Hongyan. *Mechanics of Materials*. First edition. Place of publication not identified: EDP Sciences, 2024. Web.

GitHub Repository for this Lab Report:

https://github.com/vendingmchne/SMD3-Structures-Lab-Report